IEEE Access
Multidisciplinary | Rapid Review | Open Access Journal

Received May 21, 2021, accepted May 31, 2021, date of publication June 11, 2021, date of current version June 22, 2021.

Digital Object Identifier 10.1109/ACCESS.2021.3088546

Brain Affective System Inspired Control Architecture: An Application to Nonlinear System

MD QUTUBUDDIN[1], TILAHUN KOCHITO GIBO[2], RAJU S. BAPI[3], (Senior Member, IEEE), AND YADAIAH NARRI[4], (Senior Member, IEEE)

[1]Electrical and Electronics Engineering, TKR College of Engineering and Technology, Telangana 500097, India
[2]Electrical and Computer Engineering, Mizan-Tepi University, Tepi 260, Ethopia
[3]Cognitive Science Laboratory, IIIT Hyderabad, Hyderabad 500032, India
[4]Electrical and Electronics Engineering, JNTUH College of Engineering Hyderabad, Hyderabad 500085, India

Corresponding authors: Tilahun Kochito Gibo (tilahunkochito94@gmail.com; tilekzd12@gmail.com) and Md Qutubuddin (qutubuddin30@gmail.com; mdqutubuddin@tkrcet.com)

This work was supported by Academic Press.

ABSTRACT This paper presents a bio-inspired intelligent controller to enhance the performance of a nonlinear system. The controller is designed by capturing the emotional intelligence of mammalian brain mediated by the limbic system in which certain parts are responsible for generating emotions and these can be combined together as brain affective system inspired control architecture (BASIC). This controller has been used to cope with nonlinearities present in control applications. In this paper brain inspired control architecture is proposed while incorporating the sensory cortex explicitly in the architecture and the computational equations of various modules are suitably developed. The performance of the proposed controller is analyzed on a typical nonlinear system, namely, Permanent magnet synchronous motor for speed control, harmonics in stator phase currents and ripples produced in electromagnetic torque at different operating conditions. Its performance is compared with the existing control techniques in offline simulations as well as in real-time Hardware-in-loop environment. The results establish the computational efficiency, accuracy and robustness of the proposed controller.

INDEX TERMS Amygdala, affective controller, limbic system, speed, torque, current.

I. INTRODUCTION

Recent developments in control theory concepts for dynamical systems namely modeling, design of controllers and their analysis emerged as potential research topics of interest [1]–[5]. Presently, there are significant advantages in control theory to develop modern controllers to obtain high performance. Biological models provide inspiration to introduce new intelligent control techniques to solve nonlinear problems and also to perform better compared to the existing controllers [6]–[8]. The cognitive model controllers mimic certain parts of the mammalian brain which are responsible for taking fast decisions [5], [6], [9]. The emotion signals are generated in the mammalian brain to reach the targeted goal very fast and accurately. Artificial emotion signals can be generated by mimicking characteristic parts involved in the limbic system and the resulting solution is referred as *brain affective system inspired control* (BASIC) architecture [3], [10], [11]. BASIC is developed to analyze nonlinear dynamical systems and as a test case, *permanent magnet synchronous machine* (PMSM) drive is chosen with vector control scheme to analyze its dynamic performance [12], [13]. Classical vector control operation is modified to control PMSM drive with constant torque angle ($\delta = 90^0$) control, which makes flux producing component (I_d) and torque producing component (I_q) equal to the supply current. Although, in precise control applications an accurate speed controller is required to overcome the air gap flux linkage effects on electromagnetic torque that cause speed variations. Proper selection of speed controller can reduce the nonlinear effects of PMSM. Classical controllers such as *proportional* (P), *proportional-integral* (PI) and *proportional-integral-derivative* (PID) based speed controllers due to their simple construction and easy functionality are used to solve the nonlinearities of PMSM drive [14]–[16]. But, the performance of controllers falls short of target (command) response due to parameter variations, change in speed and sudden load variations of PMSM drive. Intelligent controllers can overcome the limitations of classical controllers to improve the performance of PMSM drive. Fuzzy logic controller, neural

The associate editor coordinating the review of this manuscript and approving it for publication was Kan Liu.

networks and their hybrid structures with classical controllers are used to solve the nonlinearities [17]–[20]. Design of such control structures requires complete behavioral information about the system and large set of training data for updating the weight parameters, thereby increase the computational complexity [21]–[24]. Evolutionary algorithms are applied on PMSM drive to solve the nonlinearities. These algorithms, on iteration, give a new solution for the problem, which may converge to suboptimal local minima or maxima [25], [26]. In view of the above, BASIC architecture is a good candidate to overcome the problems associated with existing control schemes and their limitations in implementation. The BASIC structure is modeled with limbic system of mammalian brain. For a particular emotional event, the amygdala in the limbic system being highly sensitive, is likely to give very fast action and the *orbitofrontal cortex* (OFC) may give more accurate action although slowly. For example, if a rope line is found on road side, the first decision of a mammal could to mistake it as a snake and after careful observation a conclusion may be arrived as it being a rope. The first decision comes from the amygdala which can be treated as feed forward model and the latter response arises from the OFC which can be treated as feedback model [27]–[29]. This dual responsive architecture can be extended to form into a controller to solve real-world applications and to apply in control engineering applications.

This paper is organized as follows: Section 2 presents related literature pertaining to this research domain. Further we briefly discuss the emotions and how to build emotion-inspired controller for engineering applications. BELBIC, an important emotional controller is also described here. Next, Section 3 we explain our approach to developing affective controller and architecture. In Section 4, the current framework and application to PMSM drive are presented. Section 5 describes the implementation of BASIC architecture in order to test it. In Section 6, the experiments conducted and the test cases considered to validate the proposed BASIC architecture in high performance applications are included. Finally, Section 7 includes conclusions.

II. RELATED WORK

A. MOTIVATION FOR AN ALTERNATIVE CONTROL MODEL

Various traditional controllers such as the *proportional* (P), *proportional-integral* (PI) and *proportional-integral-derivative* (PID) based control schemes are classical and have been effectively utilized in many applications [14]–[16]. The design of these conventional controllers are primarily implemented using error signal that is estimated by comparing the target and the current states of the system and subsequently reducing the error to reach the expected goal. As such, the design of these controllers remains error-prone because of their inability to cope with dynamic changes in the plant and the external conditions of the environment. The design of artificial intelligent controllers include more number of input values as well as monitoring errors and their rate of change to accomplish operation even with environmental perturbations. These intelligent schemes further motivate us to design

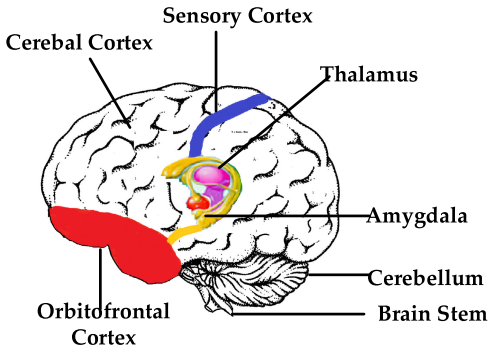

FIGURE 1. Mammalian brain and connections of amygdala.

affective controllers using inspiration from the mammalian brain. The design of affective controller requires two to three inputs and contains affective learning mechanism to arrive at accurate decisions for the problems encountered.

B. THE AFFECTIVE SYSTEM OF THE BRAIN

The mammalian brain with limbic system and its associated parts is shown in Fig. 1. The amygdala, an almond-shaped organ shown in Fig. 1, plays a vital role in decision making process by virtue of its connections with other sensory parts of the brain. The *Orbitofrontal Cortex* (OFC) is located in the lower portion of the frontal lobe of the mammalian brain. OFC, in association with amygdala, plays a key role in decision making process mediated by the limbic system. The combination of amygdala and OFC enhances learning and the emotional capability of the mammalian brain to respond quickly. In the current framework, the *Sensory Cortex* (SC) is conceptualized as a generic module that processes various kind of sensory information and that it has internal connections with amygdala and OFC to respond quickly. The proposed SC module is distributed over several cortical and sub-cortical regions of the mammalian brain and participates in sensing and transmitting of primary sensory information. In the proposed architecture, the functionality of the parts of the limbic system is modeled into a controller. Thus by modeling parts of the limbic system with mathematical functions, fast decisions could be generated in control engineering applications when compared to conventional controllers.

C. HOW EMOTIONAL SYSTEM CAN BE VIEWED AS A CONTROLLER?

The brain anatomy reveals that emotions play a major role to take early action in the problems experienced. The Limbic system of mammalian brain is responsible to generate emotions to finish or attend to the task in all complex situations. The mammalian brain is not a simple organ of body but have complex structure that acts as a responsible gateway for all actions of organs due to their interconnections with the brain [7], [3], [5], [6], [11], [4]. This interaction is made possible by virtue of emotions, thoughts and all the experiences of the organism. The mammalian brain is adapted to learn with experience based on conditioning. The limbic system

parts seem to act together as a multi-agent system. These parts depend on each other to learn emotions and give appropriate signals to the organism whenever a quick decision is to be taken. The decision making capability of the limbic system inspired researchers to mimic as a computational model for real world applications.

Previously, imitative learning process is taken into consideration to develop computational models of biological systems. In imitation learning, knowledge is transferred from one agent to other agent through the mechanism of mentor-mentee model [3], [5], [6], [10], [11]. Some of the limitations of imitation learning process are that the learning is limited to accomplishing similar results as the mentor and the absence of adaptability. However, the mimicking algorithms can be implemented in biological brains seem to have the capability of learning, adaptability as well as generalization beyond the training examples. The main aim in this work is to develop a parameter-learning adaptability to achieve improved performance for control of nonlinear system. Emotional intelligence is modeled by mimicking the limbic system of the mammalian brain, combining the structure of amygdala and orbitofrontal cortex (OFC) systems. The neural structure of amygdala and OFC are responsible for taking fast decisions on the basis of emotional learning. Moren and Balkenius [30], after several attempts, developed a computational network model of the limbic system. These network models comprise amygdala and orbitofrontal cortex as learning modules, while thalamus and sensory cortex are associated with input functions.

D. BRAIN EMOTIONAL LEARNING BASED INTELLIGENT CONTROLLER (BELBIC)

Lucas *et al.* [31] had extended the computational model of Moren and Balkenius and named it as *brain emotional learning based intelligent controller* (BELBIC) and utilized for several control applications. Rahman *et al.* [32] used BELBIC to control 1 hp Interior PMSM (IPMSM) drive and implemented in real time. Sharbafi *et al.* [33] used the BELBIC technique for motion control of an omni-directional robot. The results obtained in simulation are compared with real time implementation to show the effectiveness of BELBIC. Roshanaei *et al.* [34] have implemented BELBIC for adaptive antenna applications to estimate the arrival direction of the incoming signals and performing adaptive beam-forming. Markadeh *et al.* [35] adapted BELBIC to control speed and flux of an Induction motor. Further Soreshjani *et al.* [36] applied this control solution to power system applications for FACTS device *Thyristor controlled series capacitance* (TCSC) for active power flow control of transmission line.

E. DESIGN OF BELBIC [32]

For concreteness, we give the technical description of BELBIC below [32]:

The sensory input (S_i) is expressed as:

$$S_i = A.U_p + B.U_p \tag{1}$$

where U_p is the plant output i.e., actual speed of motor (ω_r), A and B are the gains of sensory signal.

The emotional cue (EC) is expressed as:

$$EC = k_1.\int edt + k_2.U_c \tag{2}$$

where, e is error in speed with respect to a reference value, i.e., $e = \omega_{ref} - \omega_r$, U_c is controller output and k_1, k_2 are the gains of emotional cue functions.

The amygdala learning model is expressed as:

$$A_i = V_i S_i \tag{3}$$

where V_i is the gain connection of amygdala and expressed as

$$\Delta V_i = \alpha.S_i.\max(0, [EC - \sum\nolimits_i A_j] \tag{4}$$

The OFC output may be written as:

$$O_i = W_i S_i \tag{5}$$

where the Wi is the gain connection of OFC and expressed as

$$\Delta W_i = \beta(E^{t-1} - EC)S_i \tag{6}$$

where $E^{t-1} = A_i(t-1) - O_i(t-1)$

The output of controller is given by

$$E = \sum\nolimits_i A_i - \sum\nolimits_i O_i \tag{7}$$

The amygdala output in Eqn. (3) shows that it has connection with sensory signal and emotional cue function. The output of amygdala is the primary emotional signal response but it contains disturbances in the generated emotional response. Consequently, the output of amygdala is subtracted from that of the OFC given by Eqn. (5) to arrive at the final emotional response signal, E as shown in Eqn. (7). In the following section, we outline how this scheme has been modified to propose our approach called, BASIC.

III. OUR APPRAOCH

The control structure of BELBIC contains sensory signal, emotional cue, amygdala and *orbitofrontal cortex* (OFC) as main elements [32]. In the existing design of BELBIC, sensory cortex and its connections are not considered and they are incorporated in a superficial way by supplying the sensory signal information to the limbic system directly. In this paper, we modify the control structure of BELBIC by including the sensory cortex and named the resulting scheme as *brain affective system inspired control* (BASIC) architecture. In this architecture we refer to sensory cortex as being responsible for five major senses namely smell, sound, taste, vision and touch as well as the proprioceptive sensory information [37]. It is to be noted that in the mammalian brain there are distinct and specialized modules for each of the senses and these modules are spatially distributed over the cortical and sub-cortical regions of the brain. For the sake of simplicity we lumped all these senses into a module called *Sensory cortex* (SC) in the BASIC architecture. The sensory information is integrated

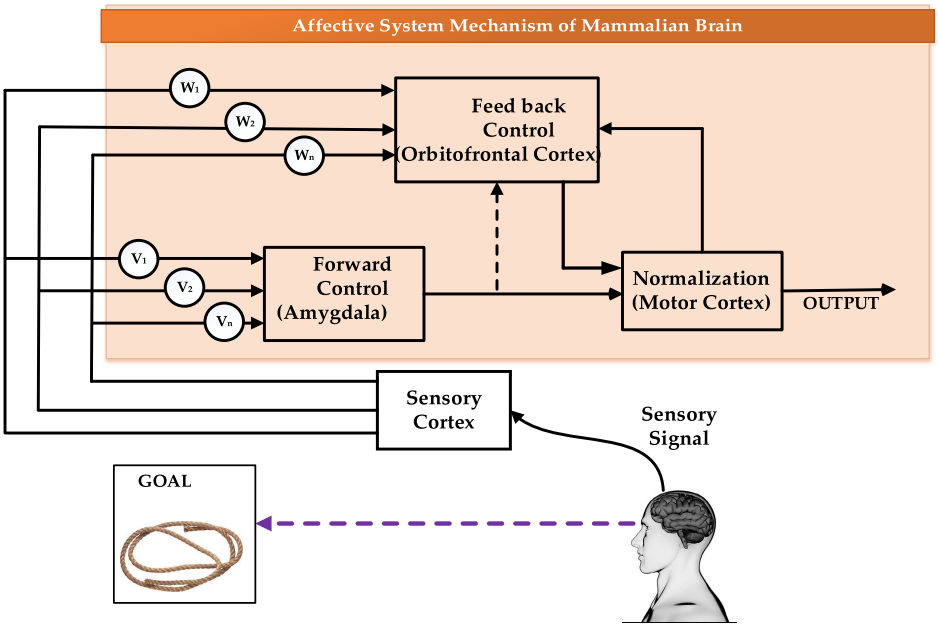

FIGURE 2. Affective system mechanism of mammalian brain.

with components of the limbic system i.e., amygdala and OFC, to generate necessary action/response in a given task. The inclusion of SC modifies the learning rate of amygdala and OFC and enables processing of information very rapidly and with accuracy.

In this paper, an application of the BASIC architecture is demonstrated in a real-world problem such as controlling of the surface mounted PMSM (SPMSM) drive to overcome limitations of the BELBIC system proposed earlier [41]. Figure 2 shows the action mechanism of the system with the inclusion of a module called the Sensory cortex. In goal-oriented action scenario, processing of sensory signal can be modeled with both feed forward and feedback mechanisms mediated by amygdala and OFC, respectively. The output of these models is normalized in the motor cortex to generate the final control response. In contrast to previous model of BELBIC [31]–[34], sensory signal was directly processed to estimate control response. In the proposed BASIC architecture, signal from the sensory cortex is explicitly included that is expected to strengthen the feed forward and feedback mechanisms and in turn improve the performance of the system compared to existing BELBIC control schemes. It can be observed from Fig. 2 that the forward model contains the weights V_1, V_2,.... V_n whereas the feedback model contains W_1, W_2,.... W_n as weights, both weights are adjusted based on the goal to be attained.

IV. PROPOSED FRAME WORK: DESIGN OF BASIC ARCHITECTURE

In the BELBIC the learning gains of amygdala and OFC are modeled with sensory input signals. The integration of SC for learning mechanism of amygdala and OFC could increase the

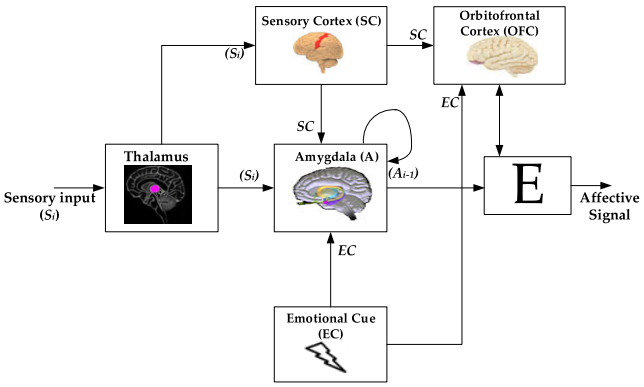

FIGURE 3. Modified BEC structure with brain parts.

signal conditioning to take swift and accurate decision. The detailed structure of BASIC along with brain areas associated with various computations is as shown in Fig. 3. The emotional signal generation is initiated with selection of sensory input signal and processed in SC. The SC is integrated with amygdala and OFC to give early emotional output signal. The emotional cue function gives necessary reward to the amygdala and OFC. The technical design details of BASIC are given below:

The sensory input (S_i) is expressed as:

$$S_i = G_1.e + G_2.U_p + G_3 \int U_c dt \tag{8}$$

where e is the speed error, U_p is plant output and Uc is controller output. G_1, G_2 and G_3 are gains of the sensory signal.

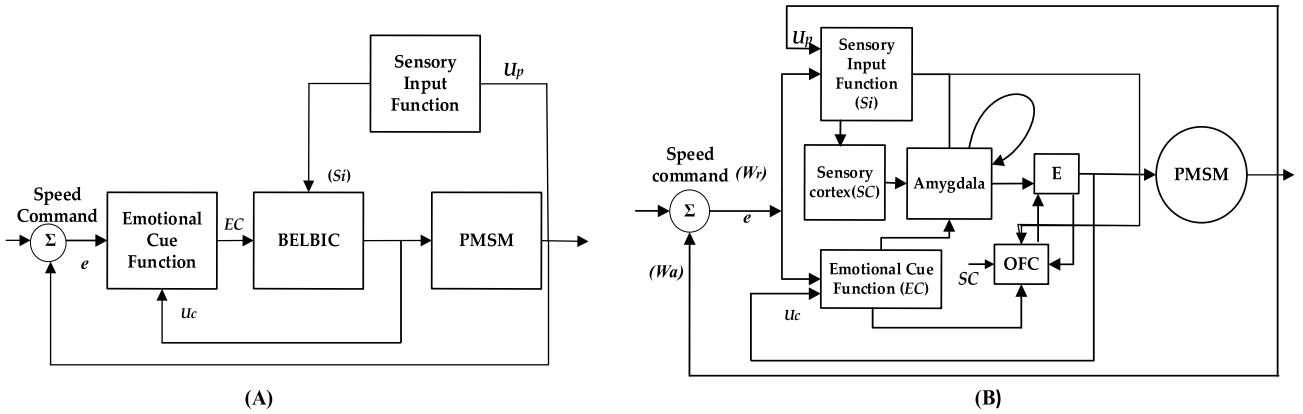

FIGURE 4. A) BELBIC architecture with plant [32] B) Proposed BASIC architecture with plant model.

The functionality of the sensory cortex (SC) is expressed as:

$$SC_i = e^{S_i} \tag{9}$$

The emotional cue (EC) is expressed as:

$$EC = a.e + b.|e.U_c| + c.U_p \tag{10}$$

where e is the speed error, U_p is plant output and U_c is the controller output. a, b and c are tunable gains of EC.

The amygdala and OFC learning models are modified as:

$$A_i = V_i S_i \tag{11}$$

where V_i is the gain connection of amygdala and expressed as:

$$\Delta V_i = \alpha.SC_i.\max(0, [EC - \sum\nolimits_i A_{j-1}] \tag{12}$$

The OFC output may be written as:

$$O_i = W_i S_i \tag{13}$$

where the Wi is the gain connection of OFC and expressed as:

$$\Delta W_i = \beta(E^{t-1} - EC)SC_i \tag{14}$$

where, $E^{t-1} = A_i(t-1) - O_i(t-1)$

The output of the controller E that stands for emotional signal can be expressed as:

$$E = \sum\nolimits_i A_i - \sum\nolimits_i O_i \tag{15}$$

The inclusion of SC signal modifies the amygdala and OFC gain connections whereas in BELBIC structure (*See section II.E),* the gain connections of amygdala and OFC contain sensory input signal. Inclusion of SC in amygdala and OFC learning models speeds up the signal conditioning to generate swift emotional response. The emotional response (E) is obtained from the outputs of amygdala and OFC. In particular, the output of amygdala A_i is always positive and if O_i is positive, it acts as inhibitor and if it is negative it acts as reinforcer. In other words, while learning sets up permanent connections between sensory cortex and amygdala; the connections from sensory cortex to OFC enable flexibility.

A. COMPARISON OF BELBIC AND BASIC

BELBIC is shown in Fig.4 (A) and the BASIC architecture proposed in this paper is shown in Fig.4 (B). Sensory cortex is stacked above emotional cue function to compute sensory input function. In addition, the computational equations for sensory input function and emotional cue functions are also modified [26]–[28].

In the BELBIC architecture SC is absent, the sensory and emotional cue functions act as input signals in the design of the amygdala and OFC learning mechanisms. However, sensory input signal is function of plant output (U_p) and emotional cue is function of error (e) and controller output (U_c). Whereas in BASIC architecture the sensory input is modified with three input values error (e), plant output (U_p) and controller output (U_c). The amygdala and OFC learning mechanisms are modified based on the SC signal. In comparison to BELBIC, in the BASIC architecture the control signal is made more compact with addition of input values. This resulted in the error becoming smaller within less time and with an increase in performance of the system as described below.

A head-to-head comparison of the performance of BELBIC and BASIC schemes is shown in Fig. 5. As can be seen from the figures, for similar output from both controllers the sensory input value required is very high (60 amps) for BELBIC. On the other hand, the sensory input required is significantly smaller (8 amps) for BASIC. Amygdala and OFC outputs are very high in the case of BELBIC. The SC output for the applied input is observed to be 0.98 amps which lower the outputs of amygdala and OFC. The results clearly indicate that sensory signal values are lowered in the case of BASIC and made the size of controller compact. This shows that proper selection of sensory signal, emotional cue and Sensory cortex signal will lower the output of amygdala and OFC to achieve the desired output. Stability analysis of the control scheme of BASIC is given in Appendix-I.

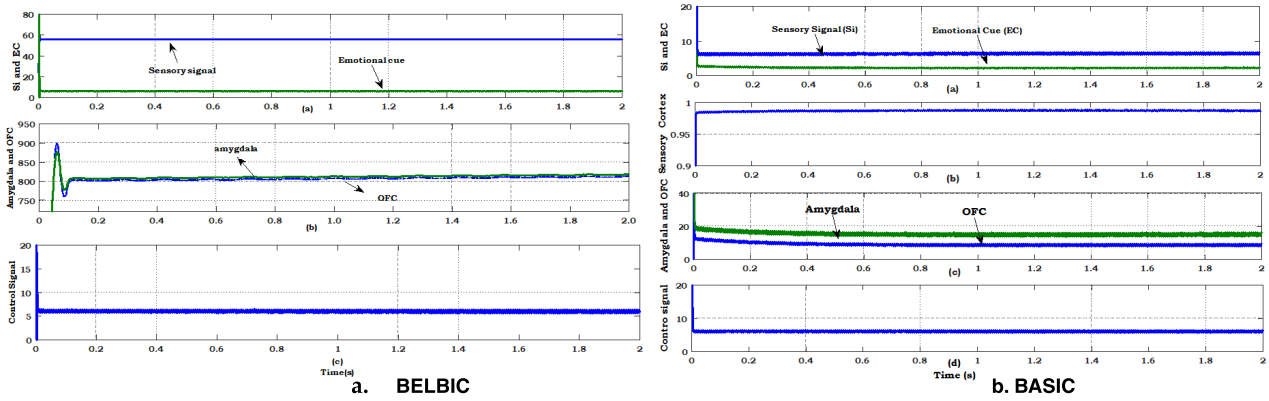

FIGURE 5. Characteristics of BEC and modified BEC.

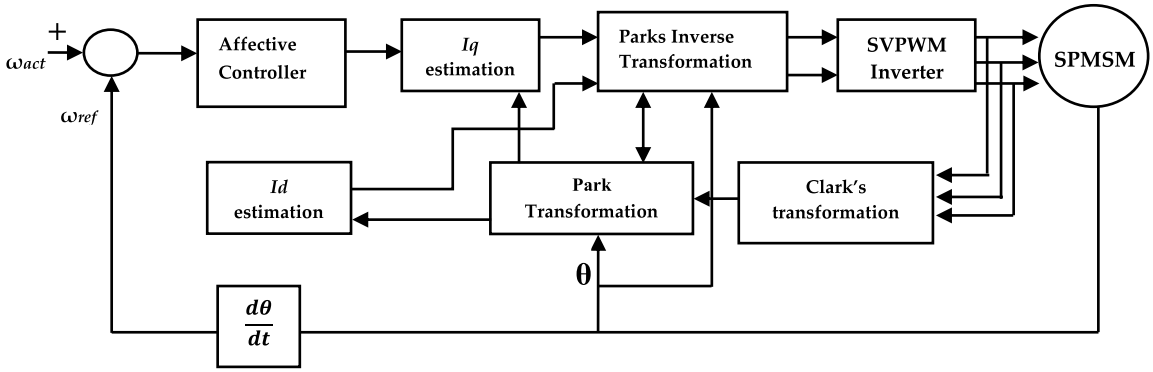

FIGURE 6. Block diagram of PMSM machine with BASIC.

B. APPLICATION OF BASIC ARCHITECTURE TO PMSM DRIVE

Fig. 6 shows the block diagram of vector control of PMSM drive with respective transformation blocks and a precise speed controller block i.e., the brain affective controller. It is to be noted that the drive is modeled in rotor reference frame [29], [4].

The design of speed controller is based on the speed error signal received from reference speed and actual speed of machine. The speed controller generates I_q value that is further transformed for estimating the final value. I_d value is estimated with the assumption of an initial $I_d = 0$. The inverter switches are tuned using *Space vector pulse width modulation* (SVPWM) technique with the help of motor phase currents. Clarke and Park transformation are used to generate required PWM signals.

1) MATHEMATICAL MODELING OF PMSM MACHINE

The mathematical modeling of PMSM drive contains electrical and mechanical parameters with *d-q* axes synchronously rotating reference frame. Modeling of PMSM machine is made with assumptions that the induced EMF is sinusoidal, damper windings are absent on rotor and that saturation and core losses are negligible [12]–[15].

$$\begin{aligned}\left[V_q V_d\right] &= \left[R_q + L_q p\omega_r L_d - \omega_r L_q R_d + L_d p\right]\left[I_q I_d\right] \\ &\quad + \left[p\omega_r \psi_f 0\right] \end{aligned} \tag{16}$$

$$T_e = \frac{3P}{2}\left[\psi_f I_q + \left(L_d - L_q\right) I_d I_q\right] \tag{17}$$

$$T_e = T_L + J_m p\omega_r + B_m\omega_r \tag{18}$$

where V_d, V_q are stator voltages, I_d, I_q are stator currents, ω_r is rotor speed, R_d, R_q are stator resistance per phase. L_d, L_q are inductance of *d-q* axes, P number of pole pairs of motor, Ψ_f is rotor magnetic flux linking the stator; T_L is load Torque; T_e is electromagnetic Torque; B_m is friction coefficient of motor; and J_m is moment of inertia of the motor. The motor parameters considered in the design of machine are listed in Table 2 of Appendix II.

In the PMSM drive, the developed toque contains ripples that lead to disturbance in the performance of vector control of PMSM drive. The motor is modeled in *d-q* axes synchronously rotating frame as shown in Eq. (17). The developed torque can be made linear with consideration of direct axis current $I_d = 0$. This control technique is called as *constant torque angle control* ($\delta = 90^0$), i.e., torque angle is maintained constant. Fig.7 shows the phasor diagram for constant torque angle control. It can be seen from the figure that the d-axis flux linkage depends on rotor magnets only and torque is maintained constant. In Eq. (18). Electromagnetic torque (T_e) epends on load, speed, friction and inertia constants in which speed and load are variables. The electromagnetic torque changes with the variations of speed and load disturbances. It is required to design a precise speed

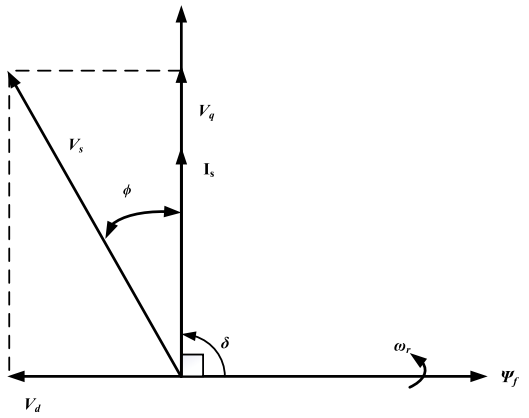

FIGURE 7. Phasor diagram for constant torque angle control.

controller that controls torque ripples. The maximum speed of rotor in this control is obtained for a given stator current (I_s) as shown in Eq. (23).

$$T_e = \frac{3P}{2}\left[\psi_f I_q\right] \tag{19}$$

$$T_e = T_L + J_m p\omega_r + B_m\omega_r \tag{20}$$

$$V_d = -p\omega_r L_q \tag{21}$$

$$pI_q = \frac{1}{L_q}\left[V_q - R_s I_s - p\omega_r\psi_f\right] \tag{22}$$

$$\omega_r\,(max) = \frac{V_s\,(max)}{\sqrt{1+\left(L_q I_q\right)^2}} \tag{23}$$

V. REALTIME IMPLEMENTATION OF THE BASIC ARCHITECTURE

The affective controller-fed PMSM drive is implemented in offline mode using MATLAB simulation as well as in real-time through *Hardware-in-loop* (HIL) with target computer configuration for performing parallel computations [38]. In this method, a complex system is divided into subsystems and all are operated at the same time. These subsystems are divided in CPU nodes which are equal to the number of subsystems. This enables to accomplish parallel distributed real time computations. In the real time implementation, driver circuit simulation includes controller, converter circuit and PMSM machine. The set-up model for real time digital simulations is shown in Fig 8.

The control techniques are modeled with simulink blocks in MATLAB and fed to simulator that converts the model into C language and generates control signal i.e., switching signals for inverter to control the drive. The time step is fixed to have a system response time of 15μs where for every interval of time step the control signal is generated. These signals can be checked with oscilloscope and also in the PC that is connected to the target. The inverter circuit is designed with *space vector pulse width modulation* (SVPWM) technique to generate switching signals to inverter that is based on *insulated gate biploar transistor* (IGBT) power devices.

These switching signals are generated based on the control signal that is generated based on speed error, controller output and plant outputs. The proposed BASIC architecture as well as BELBIC and PI controllers are implemented for PMSM drive. Different tests have been conducted to analyze their relative performance on the same nonlinear control problem.

VI. RESULTS AND DISCUSSIONS

To investigate the performance of the proposed BASIC architecture and to establish its effectiveness in comparison to other control schemes, all have been implemented on PMSM drive. Tests were conducted at different operating conditions, i.e., constant speed, change in reference speed and change in load conditions. The BASIC results are validated by comparing with BELBIC and classical PI controller. The control schemes are firstly tested in Offline simulation and then implemented in real time HIL environment.

A. OFFLINE SIMULATIONS

Offline simulation tests are conducted in MATLAB Simulink environment. Fig. 9 shows the simulation results of PMSM drive at constant speed of 300 rad/s with constant load of 5 N-m. In Fig. 9 (a) the speed tracking of PMSM drive with BASIC settles to commanded speed of 300 rad/s very smoothly and swiftly without any oscillations but with BELBIC (Fig. 9 middle column), the motor speed attains commanded speed with transient oscillations, peak overshoot is observed and time taken to reach the speed is high. Similar observations can be seen with PI based controller as shown in Fig. 9 (last column). Here, the speed takes more time to reach the reference commanded compared to BASIC and BELBIC controllers.

The speed response of all the three controllers is shown in Fig.10. It clearly shows that the speed response time of BASIC-fed PMSM drive is 0.0025s whereas with BELBIC is 0.0055s and 0.015s for PI controller with peak overshoot and transient oscillations. Fig. 9 (b) gives the waveform of stator phase currents of PMSM machine.

From the figures it can be observed that BASIC-based PMSM drive gives less harmonic distortion with 7.86% against 12.95% with BELBIC and 13.33% with PI control scheme. Fig. 9(c) shows that electromagnetic torque ripple variations are observed with a magnitude of 7.69% for BASIC as against 8.80% and 9.45% for BELBIC and PI control techniques, respectively. The effectiveness of the controllers is tested by conducting speed tracking test for PMSM drive. Fig. 11 shows speed tracking performance with speed command signals of 200-300-(-200)-(-300) rad/s at the time intervals of 0-0.4-1-1.5s. Based on speed response depicted in Fig. 11 (a), it can be seen that there are no transients and peaks can be seen that there are no transients and peaks observed in speed response of BASIC. In contrast, speed oscillations are observed at starting and when change of speed is applied in the case of existing control techniques. The stator winding draws more current for existing control techniques whereas the same is reduced in the case of affective control

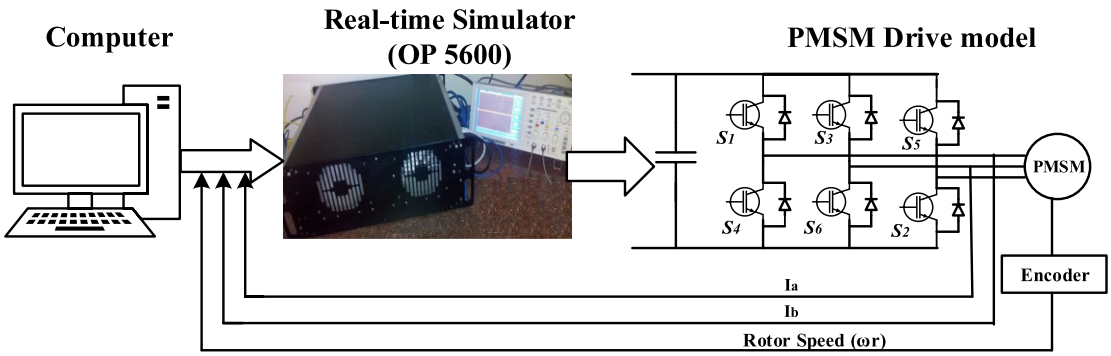

FIGURE 8. Real-time set up model.

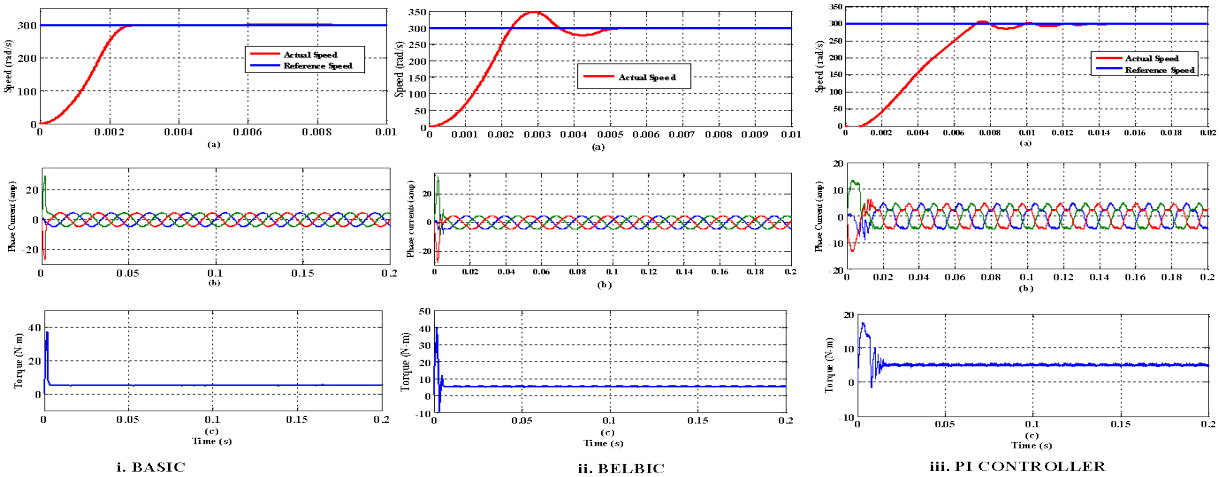

(a) Speed, (b) Stator Phase Currents and (c) Electromagnetic Torque

FIGURE 9. Simulation results of PMSM drive at constant speed.

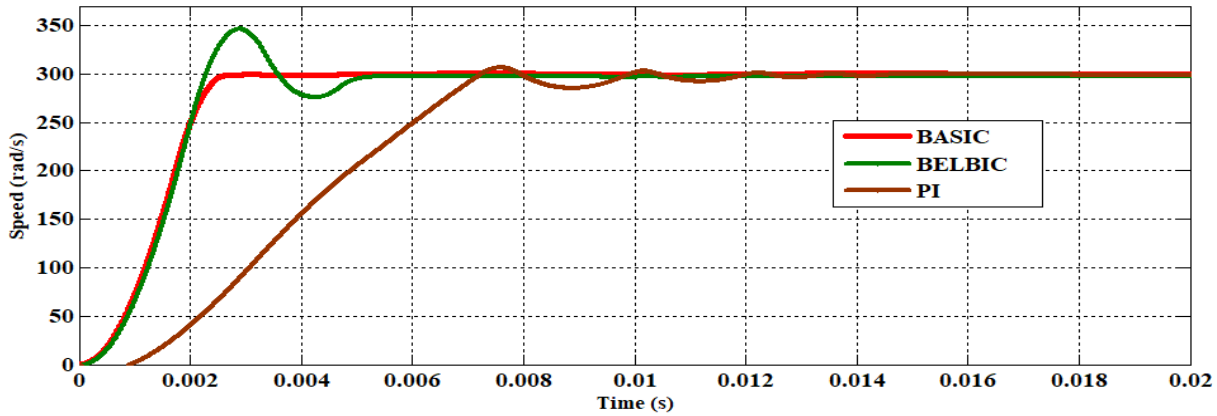

FIGURE 10. Comparison of speed response PMSM drive with BEC and MBEC.

technique as shown in Fig. 11 (b). The torque variations are high in BELBIC and PI control techniques as compared to BASIC (See Fig.11 c).

The dynamic loading capability of PMSM drive is tested by sudden application of load disturbance of 5N-m at 0.5s as shown in Fig.12. When a sudden load is applied on the motor, change in speed response is observed in the shape of a small dip. The time taken to recover from load change is high for BELBIC and PI control architectures. The corresponding effect on stator winding draws more currents with respect

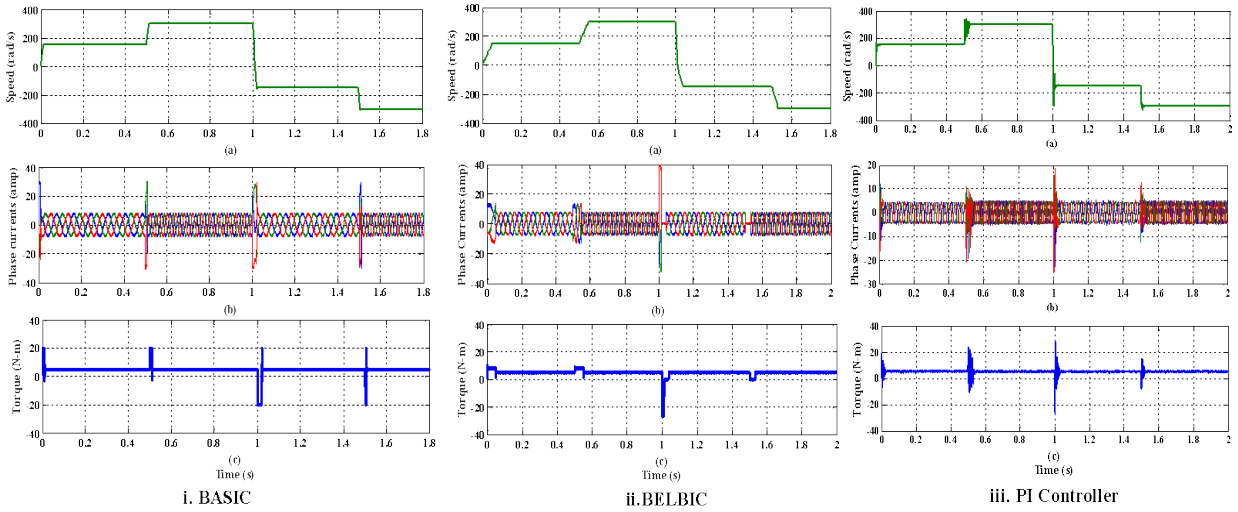

(a) Speed, (b) Stator Phase Currents and (c) Electromagnetic Torque

FIGURE 11. Simulation results of PMSM drive at variable speed.

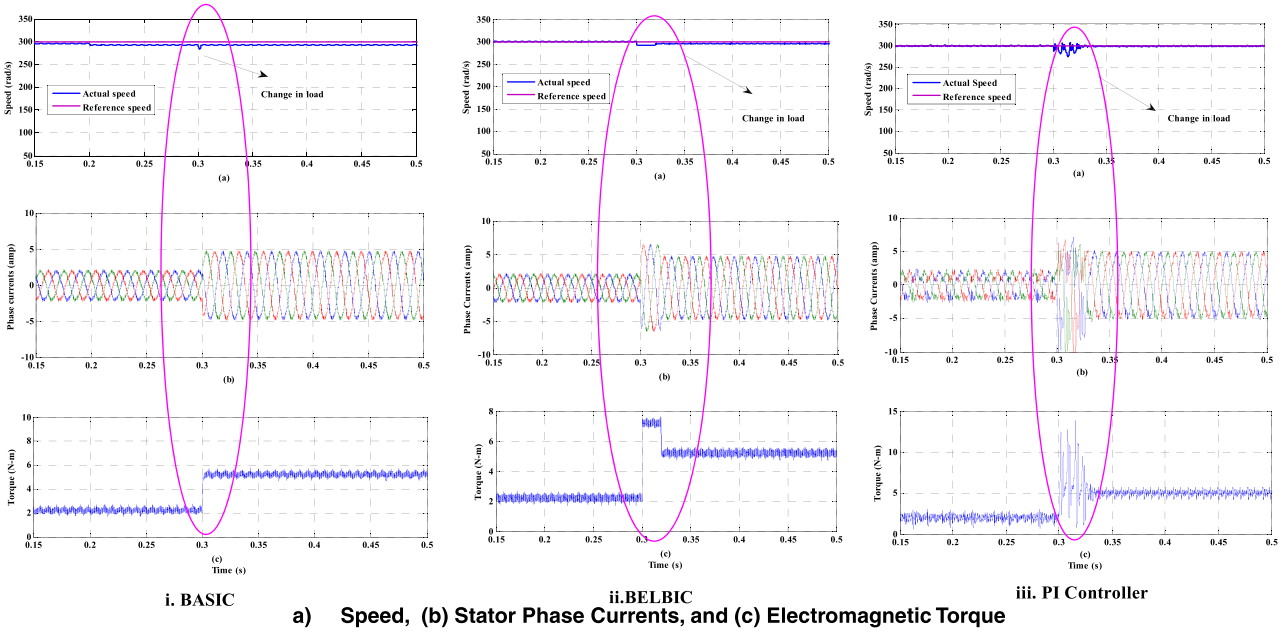

a) Speed, (b) Stator Phase Currents, and (c) Electromagnetic Torque

FIGURE 12. Simulation results of PMSM drive at variable load.

to load change. The generation of electromagnetic torque attained for a new value of applied load from 2N-m to 5N-m for which more torque ripples are found with BELBIC and PI control architectures.

B. REAL-TIME EXPERIMENTATION RESULTS

The performance of the proposed method in offline simulations is validated experimentally by conducting real time experiments using OP 5600 HILbox. Fig.13 shows constant speed tracking performance of PMSM drive for the reference speed of 300 rad/s. BASIC gives faster response with fewer variations as seen in Fig. 13 (a), with settling time of 0.008s against 0.015s and 0.02s of settling time for BELBIC and PI controllers, respectively.

The speed response of the three controllers is shown in Fig. 14. The stator phase variations are shown in Fig. 13(b) and the total harmonic distortion (THD) observed to be 9.49% as against 15.38% for BELBIC and 16.44% for PI controller-based PMSM drive. The torque production is shown in Fig. 13 (c) with the torque ripples of 18.57% and with BELBIC and PI controller the torque ripples are observed to be 22.35% and 27.04%, respectively. The PMSM drive is operated in

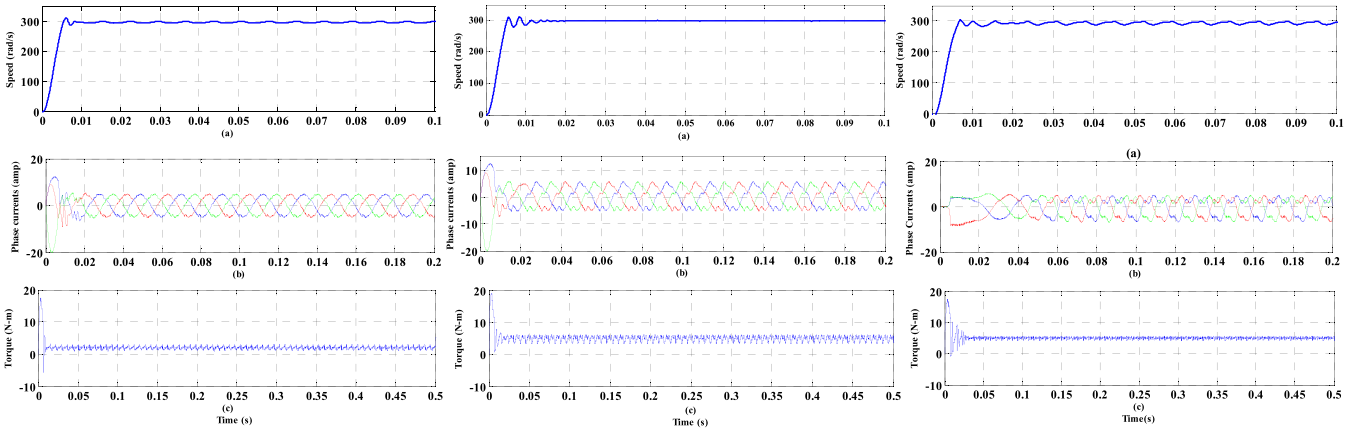

(a) Speed, (b) Stator Phase Currents, and (c) Electromagnetic Torque

FIGURE 13. Real-time results of PMSM drive at constant speed.

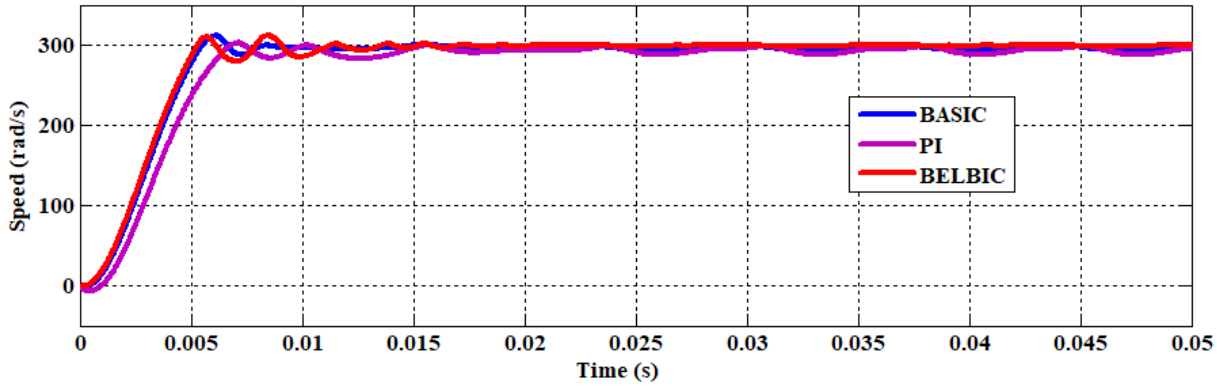

FIGURE 14. Comparison of speed response PMSM drive with BASIC and BELBIC.

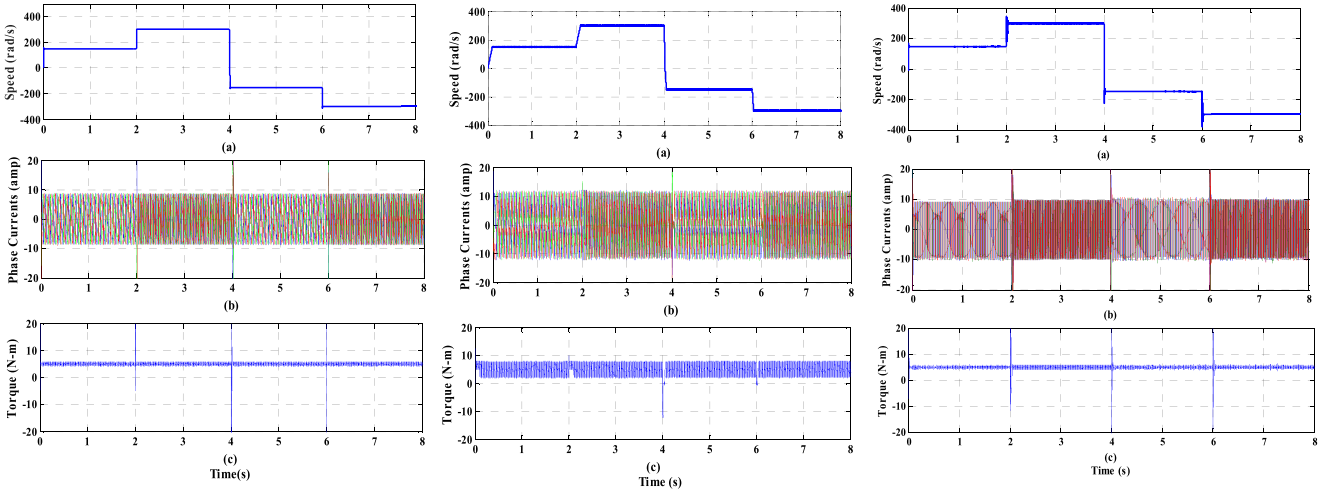

(a) Speed (b) Stator Phase Currents and (c) Electromagnetic Torque

FIGURE 15. Real-time results of PMSM drive at variable speed.

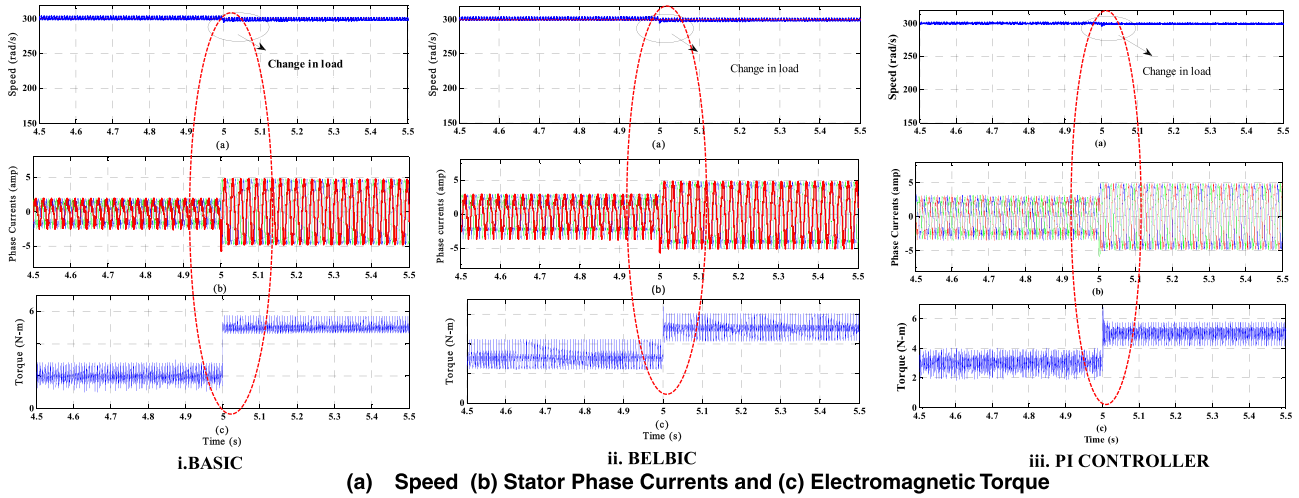

FIGURE 16. Real-time results of PMSM drive at variable load.

TABLE 1. Comparison of speed response characteristics.

PMSM response	BASIC		BELBIC		PI	
	Offline	Real time	Offline	Real time	Offline	Real time
Settling time (s)	0.0025	0.008	0.0055	0.015	0.015	0.02
Current THD (%)	7.86	9.49	12.95	15.38	13.33	16.44
Torque ripples (%)	7.69	18.57	8.80	22.35	9.45	27.04

different operating speeds of 200-300-(-200)-(-300) rad/s as tested in simulations. Although, BELBIC and PI controllers took more time to reach the command speed as shown in Fig. 15. The speed variations are impacted on the stator phase currents and electromagnetic torque produced.

The variations are shown in the figures. Overall, it is observed that BASIC-based PMSM drive gives efficient and effective results. The test results related to dynamic loading capability of controllers is shown in Fig.16 with sudden load variation of 2N-m to 10N-m. While all the three controllers are capable of handling load variations, in the case of BELBIC and PI control techniques the speed variations are more. The stator currents and torque ripples variations is shown in Fig. 16 (b)–16 (c). The variations in stator currents and in torque ripples are more for existing controllers compared to BASIC. The speed, current THD and torque ripple of electromagnetic torque observations of BASIC are compared with BELBIC and PI controllers' response, low steady state error and sensitivity to disturbance in load conditions.

Table 1 summarizes the comparisons for offline and real time observations. The summary highlights the effective performance and capability of BASIC architecture in all the test conditions. It is seen that BASIC exhibits faster response, low steady state error and sensitivity to disturbance in load conditions.

VII. CONCLUSION

In this paper a new structure called, brain affective system inspired controller (BASIC) is presented where the sensory cortex is explicitly incorporated and computational equations are modified. The performance of PMSM drive using BASIC is compared with BELBIC architectures and PI controllers in simulation and in real-time environment with different test conditions. The BASIC gives superior performance in terms of less settling time for speed with reduced overshoots, reductions in the harmonics o9f stator phase currents and reduction in ripples of electromagnetic torque produced. The BASIC contains different set of gain values which give freedom to set in to achieve required output. This inherent feature makes BASIC transient free and robust to obtain high performance. Various other application domains such as in Power system control could be explored in future. Currently internal parameters such as sensory signal, emotion cue function, etc., have been estimated by trial and error for best performance, adaptive tuning schemes for the same could be explored in the future.

APPENDIX-I

STABILITY ANALYSIS OF BRAIN AFFECTIVE SYSTEM INSPIRED CONTROL ARCHITECTURE (BASIC)

The *Brain affective system inspired Control architecture* (BASIC) is designed with various modules such as sensory signal, sensory cortex, thalamus, emotional cue, amygdala and orbitofrontal cortex. The input signals given to these modules interact among each other and interestingly become nonlinear when transformed by multiple variable functions. The sensory signal and emotional cue functions play a key role in emotional signal generation mechanism, so it is required to design them with effective functions. The stability of BASIC is obtained with sensory input and emotional cue functions because they act as input signals to amygdala and

OFC learning models. If the sensory input and emotional cue functions are stable then the BASIC is said to be stable [39], [40].

The sensory input and emotional cue functions (Eq.A.1 & Eq.A.2) are recalled to find stability

$$\begin{aligned} S_i &= f(e, U_P, U_c) \\ S_i &= G_1.e + G_2.U_p + G_3 \int U_c dt. \end{aligned} \tag{A.1}$$

$$\begin{aligned} EC &= h(e, U_P, U_c) \\ EC &= a.e + b.|e.U_c| + c.U_p. \end{aligned} \tag{A.2}$$

In order to find stability of BASIC, the equilibrium point for Eq. (A.1) and Eq. (A.2) need to be found and it must be locally stable.

The sensory input and emotional cue functions are expressed with e, U_p and U_c as variables and formed into a nonlinear model. The three variables of nonlinear model can be represented in the form as:

$$\begin{aligned} e\,(t+1) &= f(e\,(t)\,, U_P\,(t)\,, U_c\,(t)) \\ U_P\,(t+1) &= f(e\,(t)\,, U_P\,(t)\,, U_c\,(t)) \\ U_c\,(t+1) &= f\,(e\,(t)\,, U_P\,(t)\,, U_c\,(t))\,. \end{aligned} \tag{A.3}$$

where f is an arbitrary function with variables e, U_p and U_c

To find the stability of nonlinear system, firstly we find the equilibrium and prove it to be locally stable. Consider, the sensory input with function f containing three variables which are unchanging at equilibrium, which can be written as $e\,(t+1) = e\,(t) = \hat{e}$, $U_c\,(t+1) = U_c\,(t) = \hat{U}_c$ and $U\,(t+1) = U_P\,(t) = \hat{U}_P$.

Let us consider that there are small deviations ε_1, ε_1 and ε_3 for $\hat{e}$, $\hat{U}_p$ and $\hat{U}_c$ respectively. The deviations can be represented $\varepsilon_1 = e\,(t) - \hat{e}$, $\varepsilon_2 = U_c\,(t) - \hat{U}_c$ and $\varepsilon_3 = U_p\,(t) - \hat{U}_p$. If the equilibrium point $(\hat{e}, \hat{U}_c, \hat{U}_p)$ is locally stable, the deviations ε_1, ε_2 and ε_3 must decay to zero as time passes (which means that $e(t) \to \hat{e}$, $U_c(t) \to \hat{U}_c$ & $U_p(t) \to \hat{U}_p$ as time passes). In order to determine whether the equilibrium is stable or not, the dynamics of ε_1, ε_2 and ε_3 are required, which can be obtained as:

$$\begin{aligned} \varepsilon_1\,(t) &= e\,(t+1) - \hat{e} \\ &= f\left(e\,(t)\,, U_p\,(t)\,, U_c\,(t)\right) - \hat{e} \\ &= f\left(\hat{e} + \varepsilon_1\,(t)\,, \hat{U}_p + \varepsilon_2\,(t)\,, \hat{U}_c\,(t) + \varepsilon_3\,(t)\right) - \hat{e}. \end{aligned} \tag{A.4}$$

$$\begin{aligned} \varepsilon_2\,(t) &= U_p\,(t+1) - \hat{U}_p \\ &= f\left(e\,(t)\,, U_p\,(t)\,, U_c\,(t)\right) - \hat{U}_p \\ &= f\left(\hat{e} + \varepsilon_1\,(t)\,, \hat{U}_p + \varepsilon_2\,(t)\,, \hat{U}_c\,(t) + \varepsilon_3\,(t)\right) - \hat{U}_p. \end{aligned} \tag{A.5}$$

$$\begin{aligned} \varepsilon_3\,(t) &= U_c\,(t+1) - \hat{U}_c \\ &= f\left(e\,(t)\,, U_p\,(t)\,, U_c\,(t)\right) - \hat{U}_c \\ &= f\left(\hat{e} + \varepsilon_1\,(t)\,, \hat{U}_p + \varepsilon_2\,(t)\,, \hat{U}_c\,(t) + \varepsilon_3\,(t)\right) - \hat{U}_c. \end{aligned} \tag{A.6}$$

Taylor series expansion is considered to describe the functionality of multiple variables and to find the equilibrium point $(\hat{e}, \hat{U}_c, \hat{U}_p)$. The Taylor series expansion of Eqn. (A.4) to Eqn. (A.6) with respect to deviations ε_1, ε_2 and ε_3 near (0,0,0) may be obtained as

$$\begin{aligned} \varepsilon_1\,(t+1) = \Big(& f\left(\hat{e}, \hat{U}_p, \hat{y}_c\right) + \frac{\partial f}{\partial e}\Big|_{e=\hat{e}, U_p=\hat{U}_p, U_c=\hat{U}_c} \varepsilon_1\,(t) \\ &+ \frac{\partial f}{\partial U_p}\Big|_{e=\hat{e}, U_p=\hat{U}_p, U_c=\hat{U}_c} \varepsilon_2\,(t) \\ &+ \frac{\partial f}{\partial U_c}\Big|_{e=\hat{e}, U_p=\hat{U}_p, U_c=\hat{U}_c} \varepsilon_3\,(t) \\ &+ \textit{high order terms}) - \hat{e} \end{aligned} \tag{A.7a}$$

$$\begin{aligned} = & \frac{\partial f}{\partial e}\Big|_{e=\hat{e}, U_p=\hat{U}_p, U_c=\hat{U}_c} \varepsilon_1\,(t) \\ &+ \frac{\partial f}{\partial U_p}\Big|_{e=\hat{e}, U_p=\hat{U}_p, U_c=\hat{U}_c} \varepsilon_2\,(t) \\ &+ \frac{\partial f}{\partial U_c}\Big|_{e=\hat{e}, U_p=\hat{U}_p, U_c=\hat{U}_c} \varepsilon_3\,(t) \\ &+ + \textit{high order terms} \end{aligned} \tag{A.7b}$$

The expression (A.7b) follows from (A.7a) with the fact that $f\left(\hat{e}, \hat{U}_c, \hat{U}_p\right) = \hat{e}$ at equilibrium. Higher-order terms in the expression are involved for higher powers of ε_1 and derivatives are evaluated at equilibrium. ε_1 is very small at equilibrium and becomes still smaller and high powers of these deviations are extremely small so that they can be ignored. The final expression can be obtained as:

$$\begin{aligned} \varepsilon_1\,(t+1) = & \frac{\partial f}{\partial e}\Big|_{e=\hat{e}, U_p=\hat{U}_p, U_c=\hat{U}_c} \varepsilon_1\,(t) \\ &+ \frac{\partial f}{\partial U_p}\Big|_{e=\hat{e}, U_p=\hat{U}_p, U_c=\hat{U}_c} \varepsilon_2\,(t) \\ &+ \frac{\partial f}{\partial U_c}\Big|_{e=\hat{e}, U_p=\hat{U}_p, U_c=\hat{U}_c} \varepsilon_3\,(t) \end{aligned} \tag{A.7c}$$

Similarly, the calculations are repeated for ε_2 and ε_3 deviations and the expressions are found to be:

$$\begin{aligned} \varepsilon_2\,(t+1) = & \frac{\partial f}{\partial e}\Big|_{e=\hat{e}, U_p=\hat{U}_p, U_c=\hat{U}_c} \varepsilon_1\,(t) \\ &+ \frac{\partial f}{\partial U_p}\Big|_{e=\hat{e}, U_p=\hat{U}_p, U_c=\hat{U}_c} \varepsilon_2\,(t) \\ &+ \frac{\partial f}{\partial U_c}\Big|_{e=\hat{e}, U_p=\hat{U}_p, U_c=\hat{U}_c} \varepsilon_3\,(t)\,. \end{aligned} \tag{A.8}$$

$$\begin{aligned} \varepsilon_3\,(t+1) = & \frac{\partial f}{\partial e}\Big|_{e=\hat{e}, U_p=\hat{U}_p, U_c=\hat{U}_c} \varepsilon_1\,(t) \\ &+ \frac{\partial f}{\partial U_p}\Big|_{e=\hat{e}, U_p=\hat{U}_p, U_c=\hat{U}_c} \varepsilon_2\,(t) \\ &+ \frac{\partial f}{\partial U_c}\Big|_{e=\hat{e}, U_p=\hat{U}_p, U_c=\hat{U}_c} \varepsilon_3\,(t)\,. \end{aligned} \tag{A.9}$$

TABLE 2. Motor parameters.

PARAMETERS	VALUE
Resistance (R)	$R_1 = 2.85$ ohm
Inductance($L_d = L_q = L$)	0.0085henry
Friction coefficient(B)	1.0e-4 NM-S
Inertia(J)	J_1 = 8e-4 kg- m^2
Poles (P)	8
Mutual flux linkage (λf)	0.1548 web-turns
Rated speed	350 rad/sec

The above expressions Eqn. (A.7) –Eqn.(A.9) can be represented in matrix form as:

$$\begin{bmatrix} \varepsilon_1(t+1) \\ \varepsilon_2(t+1) \\ \varepsilon_3(t+1) \end{bmatrix} = \begin{bmatrix} \frac{\partial f}{\partial e} & \frac{\partial f}{\partial U_p} & \frac{\partial f}{\partial U_c} \\ \frac{\partial f}{\partial e} & \frac{\partial f}{\partial U_p} & \frac{\partial f}{\partial U_c} \\ \frac{\partial f}{\partial e} & \frac{\partial f}{\partial U_p} & \frac{\partial f}{\partial U_c} \end{bmatrix} \begin{bmatrix} \varepsilon_1(t) \\ \varepsilon_2(t) \\ \varepsilon_3(t) \end{bmatrix} \quad \text{(A.10)}$$

The matrix is a *Jacobian matrix* and is also referred to as the *stability matrix*. The system of equations is linear with three deviations ε_1, ε_2 and ε_3. Thus, (A.10) describes the nonlinear dynamics in terms of linear equations near equilibrium of interest. If the deviations $\varepsilon_1, \varepsilon_2$ and ε_3 decay to zero over time, then the equilibrium is locally stable. Conversely, if the deviations $\varepsilon_1, \varepsilon_2$ and ε_3 grow over time, then the equilibrium is unstable. Specifically, the equilibrium is stable if the absolute value of every Eigenvalue of the Jacobian is less than one, i.e., ($|\lambda_1| < 1$, $|\lambda_2| < 1$ and $|\lambda_3| < 1$). For the implemented system, the estimates of the Eigenvalues are found to be $|\lambda_1| = 0.7714$, $|\lambda_2| = 0.1070$ and $|\lambda_3| =$ -0.0484, when the appropriate values are substituted and eigen analysis is performed on the Jacobian matrix in Eq (A.10).

Similarly, to find the stability of the EC function the above method is repeated to find the stability matrix to find the Eigenvalues and they are found to be $|\lambda_1| = 0.11$, $|\lambda_2| = 0$ and $|\lambda_3| = 0$. Since the Eigenvalues are within the limits, it can be concluded that the equilibrium is stable for perturbations in S_i and EC. Hence, the BASIC scheme is a stable one with the chosen values of Sensory signal and emotional cue functions.

APPENDIX-II

See Table 2.

APPENDIX-III

The sensory signal and emotional cue gain parameters for are tuned using trial and error method and found to be 0.08, 0.05 and 0.7 for sensory input and 0.04, 0.06 and 0.01 for emotional cue respectively. The amygdala and OFC learning rates are found to be 0.08 and 0.03 respectively.

APPENDIX -IV

Stability analysis of PMSM drive can be proved using Eq. (16) and Eq. (18) can be rewritten a

$$\begin{aligned} \frac{dI_d}{dt} &= \frac{(V_d - RI_d + \omega L_q I_q}{L_d} \\ \frac{dI_q}{dt} &= \frac{(V_q - RI_q - \omega L_d I_d + \omega\psi_f)}{L_q} \\ \frac{d\omega}{dt} &= \frac{p\psi_f I_q + p\left(L_d - L_q\right) I_d I_q - T_L - B\omega}{J} \end{aligned} \quad \text{(B.1)}$$

After applying affine transformation and time scaling transformation

$$\begin{aligned} \frac{d\bar{I}_d}{dt} &= -\frac{L_q}{L_d}\bar{I}_d + \bar{\omega}\bar{I}_q + \overline{V}_d \\ \frac{d\bar{I}_q}{dt} &= -I_q - \bar{\omega}\bar{I}_d + K_1\bar{\omega} + \overline{V}_d \\ \frac{d\bar{\omega}}{dt} &= K_2\left(\bar{I}_q - \bar{\omega}\right) + K_3\bar{I}_d\bar{I}_q - \overline{T}_L \end{aligned} \quad \text{(B.2)}$$

where $K_1 = \frac{P\psi_f^2}{RB}$; $K_2 = \frac{L_q B}{RJ}$; $\overline{V}_q = \frac{PL_q\psi_f V_q}{R^2 B}$; $\overline{V}_d = \frac{PL_q\psi_f V_d}{R^2 B}$; $K_3 = \frac{L_q B^2(L_d - L_q)}{L_d JP\psi_f^2}$; $\overline{T}_L = \frac{L_q^2 T_L}{R^2 J}$

Stability analysis of PMSM

The inherent characteristics of PMSM drive with smooth air-gap can be expressed as with assumptions since the chosen PMSM drive surface mounted type.

$$\begin{aligned} L_d &= L_q; \overline{V}_d = 0; \overline{V}_q = 0; \text{ and } \overline{T}_L = 0 \\ \frac{d\bar{I}_d}{dt} &= -\bar{I}_d + \bar{\omega}\bar{I}_q \\ \frac{d\bar{I}_q}{dt} &= -I_q - \bar{\omega}\bar{I}_d + K_1\bar{\omega} \\ \frac{d\bar{\omega}}{dt} &= K_2\left(\bar{I}_q - \bar{\omega}\right) \end{aligned} \quad \text{(B.3)}$$

In order to study the dynamic characteristics of PMSM drive the parameters K_1 & K_2 are assumed to be independent. The actual dynamic behavior of drive can be obtained by substituting the actual parameters.

The equilibrium points ($\bar{i}_{do}, \bar{i}_{qo}, \bar{\omega}_o$) is analyzed by (B.4), as shown at the bottom of the next page.

(1) If $K_1 > 1$, the system have the equilibrium points including (0,0,0),

$$(K_1 - 1, \sqrt{K_1 - 1}, \sqrt{K_1 - 1}) \text{ and } (K_1 - 1, -\sqrt{K_1 - 1}, -\sqrt{K_1 - 1}).$$

(2) If $K_1 \leq 1$, the system would only have one equilibrium point (0,0,0).

The local stability of the equilibrium point is determined by the roots of the characteristic equation and the equilibrium point is stable if all the roots of the characteristics equation have negative real parts. The characteristic equation can be expressed as de $(\lambda I - J) = 0$, where λ, I and J represent the eigen value, identity matrix and Jacobian matrix respectively. In fact, the stability of the equilibrium point is usually judged using R-H stability criterion.

As solving the characteristic equation is very difficult for high dimensional dynamical system.

The jacobian matrix at the equilibrium point of system

$$J = \begin{bmatrix} -1 & \overline{\omega}_0 & \overline{I}_{qo} \\ -\overline{\omega}_0 & -1 & -\overline{I}_{do} + K_1 \\ 0 & K_2 & -K_2 \end{bmatrix} \tag{B.5}$$

Substituting the jacobian matrix and equilibrium point $(\overline{\omega}_0^2, \overline{\omega}_0, \overline{\omega}_0)$ into the characteristic equation det(λI-J) = 0,

$$\lambda^3 + (K_2+2)\lambda^2 + \left(1 + K_2\overline{\omega}_0^2 - K_2K_1 + 2K_2\right)\lambda + 3K_2\overline{\omega}_0^2 - K_2K_1 + K_2 = 0 \tag{B.6}$$

According to R-H stability criterion the sufficient condition on the local stability of the equilibrium point is

$$\begin{aligned} K_2 &> -2;\ 3K_2\overline{\omega}_0^2 - K_2K_1 + K_2 \\ &> 0\,(K_2+2)\left(1 + K_2\overline{\omega}_0^2 - K_2K_1 + \overline{\omega}_0^2 + 2K_2\right) \\ &\quad -(3\overline{\omega}_0^2 + K_1 - 1)K_2 > 0 \end{aligned} \tag{B.7}$$

Equilibrium points can be found stability using bifurcation theory. The equilibrium points may lose stability when the parameters pass through the ley values and the bifurcation behavior occurs. In order to obtain the conditions of the Hopf bifurcation, setting $\lambda = nj\,(n \neq 0)$ and substituting into characteristics equation we obtain.

$$-n^3 j - (K_2+2)n^2 + \left(1 + K_2\bar{\omega}_0^2 - K_2K_1 + \bar{\omega}_o^2 + 2K_2\right)nj + 3K_2\bar{\omega}_o^2 - K_1K_2 + K_2 = 0 \tag{B.8}$$

By equating real and imaginary parts

$$\begin{aligned} n^2 &= 1 + K_2\bar{\omega}_o^2 - K_2K_1 + \bar{\omega}_o^2 + 2K_2 \\ n^2 &= \frac{(3K_2\bar{\omega}_o^2 - K_2K_1 + K_2)}{K_2+2} \end{aligned} \tag{B.9}$$

According to the Hopf bifurcation the equilibrium point must satisfy the following conditions.

$$\begin{aligned} K_2 + 2 &> 0, \\ 1 + K_2\bar{\omega}_o^2 - K_1K_2 + \bar{\omega}_o^2 + 2K_2 &> 0, \\ \left(-K_2^2 - 2\right)\bar{\omega}_o^2 + (K_1-2)K_2^2 + (K_1-4)K_2 - 2 &= 0. \end{aligned} \tag{B.10}$$

In addition, if $K_1 > 1$, system (3) would have two stable equilibrium points and one unstable equilibrium point and if $K_1 < 1$, system (3) would only have one stable equilibrium point and the pitchfork bifurcation occurs at $K_1 = 1$.

B. When considering the external load, namely, $L_d = L_q, \overline{V}_d = 0, \overline{V}_q = 0$, and $\overline{T}_L \neq 0$, this is a special case that the control inputs of the system are removed after the motor runs for a period of operation. Let $V = \overline{T}_L$, and the system (2) becomes

$$\begin{aligned} \frac{d\bar{I}_d}{d\bar{t}} &= -\bar{I}_d + \bar{\omega}\bar{I}_q, \\ \frac{d\bar{I}_q}{d\bar{t}} &= -\bar{I}_q - \bar{\omega}\bar{I}_d + K_1\bar{\omega}, \\ \frac{d\bar{\omega}}{d\bar{t}} &= K_2\left(\bar{I}_q - \bar{\omega}\right) - u. \end{aligned} \tag{B.11}$$

By analyzing the equilibrium points, $\left(\bar{I}_{d_0}, \bar{I}_{q_0}, \bar{\omega}_0\right)$ of system (11) we obtain (B.12), as shown at the bottom of the page.

According to the relationship between $\bar{I}_{do}, \bar{I}_{qo}, and \bar{\omega}_0$ the equilibrium point of (B.11) can be written as $\left(\overline{\omega}_0^2 + u\frac{\bar{\omega}_0}{K_2}, \overline{\omega}_0 + \frac{u}{K_2}, \overline{\omega}_0\right)$. The Jacobian matrix at equilibrium point is

$$J = \begin{bmatrix} -1 & \overline{\omega}_0 & \overline{I}_{qo} \\ -\overline{\omega}_0 & -1 & -\overline{I}_{do} + K_1 \\ 0 & K_2 & -K_2 \end{bmatrix} \tag{B.13}$$

$$\lambda^3 + a_1\lambda^2 + a_2\lambda + a_3 = 0, \tag{B.14}$$

where

$$\begin{aligned} a_1 &= K_2 + 2 \\ a_2 &= (1+K_2)\,\overline{\omega}_0^2 + u\overline{\omega}_0 + (2-K_1)K_2 + 1 \\ a_3 &= 3K_2\overline{\omega}_0^2 + u\overline{\omega}_0 + (u - K_1 + 1)K_2. \end{aligned} \tag{B.15}$$

According to R-H criteria, the local stability condition of the equilibrium can be written as

$$\begin{aligned} K_2 + 2 &> 0 \\ 3K_2\overline{\omega}_0^2 + u\overline{\omega}_0 + (u - K_1 + 1)K_2 &> 0 \\ K_2\left(2 + 2K_2 + (K_2+2)\,\overline{\omega}_0^2 + u\overline{\omega}_0 - K_1\,(K_2+1)\right) + 2 &> 0. \end{aligned} \tag{B.16}$$

$$\begin{cases} -\bar{I}_{do} + \overline{\omega}_o\bar{I}_{qo} = 0 \\ -\bar{I}_{qo} - \overline{\omega}_o\bar{I}_{do} + K_1\overline{\omega}_0 = 0 \\ K_2(\bar{I}_{qo} - \overline{\omega}_0) = 0 \end{cases} \Longrightarrow \begin{cases} \bar{I}_{do} = \bar{\omega}_0^2 \\ \bar{I}_{qo} = \bar{\omega}_0 \\ \bar{\omega}_0\left(\bar{\omega}_0{}^2 - K_1 + 1\right) = 0 \end{cases} \tag{B.4}$$

$$\begin{cases} -\bar{I}_{do} + \overline{\omega}_0\bar{i}_{do} = 0 \\ -\bar{I}_{qo} - \overline{\omega}_0\bar{I}_{do} + K_1\overline{\omega}_0 = 0 \\ K_2(\bar{I}_{qo} - \overline{\omega}_o) = 0 \end{cases} \Longrightarrow \begin{cases} \bar{I}_{do} = \bar{\omega}_0^2 + \frac{u\bar{\omega}_0}{K_2} \\ \bar{I}_{qo} = \bar{\omega}_0 + \frac{u}{K_2} \\ \bar{\omega}_0{}^3 + \frac{u}{K_2}\omega_0{}^2 + (1-K_1)\,\bar{\omega}_0 - \frac{u}{K_2} = 0. \end{cases} \tag{B.12}$$

If Fold bifurcation occurs at the equilibrium point of (B.11), the following conditions must be satisfied

$$\begin{aligned} \overline{\omega}_0^3 + \frac{u}{K_2}\omega_0^2 + (1-K_1)\,\overline{\omega}_0 + \frac{u}{K_2} &= 0 \\ 3K_2\overline{\omega}_0^2 + u\overline{\omega}_0 + (u - K_1 + 1)\,K_2 &= 0. \end{aligned} \tag{B.17}$$

In Hopf bifurcation occurs at the equilibrium point of (B.11), the following conditions must be satisfied.

$$\begin{aligned} K_2 + 2 &> 0 \\ (1+K_2)\,\overline{\omega}_0^2 + u\overline{\omega}_0 + (2-K_1)\,K_2 + 1 &> 0 \\ \overline{\omega}_0^3 + \frac{u}{K_2}\omega_0^2 + (1-K_1)\,\overline{\omega}_0 + \frac{u}{K_2} &= 0 \\ K_2(2 + 2K_2 + (K_2+2)\,\overline{\omega}_0^2 + u\overline{\omega}_0 - K_1\,(K_2+1) + 2 &= 0. \end{aligned} \tag{B.18}$$

REFERENCES

[1] R. Bellman and R. Kalaba, *Dynamic Programming and Modern Control Theory* (London Mathematical Society Monographs). London, U.K.: Academic, 1965.

[2] K. Zhou, J. C. Doyle, and K. Glover, *Robust and Optimal Control*. Englewood Cliffs, NJ, USA: Prentice-Hall, 1996.

[3] J. He, M. G. Maltenfort, Q. Wang, and T. M. Hamm, "Learning from biological systems: Modeling neural control," *IEEE Control Syst. Mag.*, vol. 21, no. 4, pp. 55–69, Aug. 2001.

[4] A. Roy, "Connectionism, controllers, and a brain theory," *IEEE Trans. Syst., Man, Cybern. A, Syst., Humans*, vol. 38, no. 6, pp. 1434–1441, Nov. 2008.

[5] D. J. Mendonca and W. A. Wallace, "A cognitive model of improvisation in emergency management," *IEEE Trans. Syst., Man, Cybern. A, Syst., Humans*, vol. 37, no. 4, pp. 547–561, Jul. 2007.

[6] B. Meuleman and K. Scherer, "Nonlinear appraisal modeling: An application of machine learning to the study of emotion production," *IEEE Trans. Affect. Comput.*, vol. 4, no. 4, pp. 398–411, Oct. 2013.

[7] P. S. Churchland and T. J. Sejnowski, *The Computational Brain*. Cambridge, MA, USA: MIT, 1992.

[8] J. M. Kivikangas and N. Ravaja, "Emotional responses to victory and defeat as a function of opponent," *IEEE Trans. Affect. Comput.*, vol. 4, no. 2, pp. 173–182, Apr. 2013.

[9] H.-I. Ahn and R. W. Picard, "Measuring affective-cognitive experience and predicting market success," *IEEE Trans. Affect. Comput.*, vol. 5, no. 2, pp. 173–186, Apr. 2014.

[10] M. A. Salichs and M. Malfaz, "A new approach to modeling emotions and their use on a decision-making system for artificial agents," *IEEE Trans. Affect. Comput.*, vol. 3, no. 1, pp. 56–68, Jan. 2012.

[11] V. Uraikul, C. W. Chan, and P. Tontiwachwuthikul, "Artificial intelligence for monitoring and supervisory control of process systems," *Eng. Appl. Artif. Intell.*, vol. 20, no. 2, pp. 115–131, Mar. 2007.

[12] R. Krishnan, *Permanent Magnet Synchronous and Brushless DC Motor Drives*. Boca Raton, FL, USA: CRC Press, 2010.

[13] A. Cataliotti, F. Genduso, A. Raciti, and G. R. Galluzzo, "Generalized PWM-VSI control algorithm based on a universal duty-cycle expression: Theoretical analysis, simulation results, and experimental validations," *IEEE Trans. Ind. Electron.*, vol. 54, no. 3, pp. 1569–1580, Jun. 2007.

[14] M.-H. Hung, L.-S. Shu, S.-J. Ho, S.-F. Hwang, and S.-Y. Ho, "A novel intelligent multiobjective simulated annealing algorithm for designing robust PID controllers," *IEEE Trans. Syst., Man, Cybern. A, Syst., Humans*, vol. 38, no. 2, pp. 319–330, Mar. 2008.

[15] J. C. Basilio and S. R. Matos, "Design of PI and PID controllers with transient performance specification," *IEEE Trans. Educ.*, vol. 45, no. 4, pp. 364–370, Nov. 2002.

[16] W. Krajewski, A. Lepschy, and U. Viaro, "Designing PI controllers for robust stability and performance," *IEEE Trans. Control Syst. Technol.*, vol. 12, no. 6, pp. 973–983, Nov. 2004.

[17] K.-Y. Cheng and Y.-Y. Tzou, "Fuzzy optimization techniques applied to the design of a digital PMSM servo drive," *IEEE Trans. Power Electron.*, vol. 19, no. 4, pp. 1085–1099, Jul. 2004.

[18] H. Zhang, M. Li, J. Yang, and D. Yang, "Fuzzy model-based robust networked control for a class of nonlinear systems," *IEEE Trans. Syst., Man, Cybern. A, Syst., Humans*, vol. 39, no. 2, pp. 437–447, Mar. 2009.

[19] Q. Liang and J. M. Mendel, "Interval type-2 fuzzy logic systems: Theory and design," *IEEE Trans. Fuzzy Syst.*, vol. 8, no. 5, pp. 535–550, Oct. 2000.

[20] S. Barkat, A. Tlemçani, and H. Nouri, "Noninteracting adaptive control of PMSM using interval type-2 fuzzy logic systems," *IEEE Trans. Fuzzy Syst.*, vol. 19, no. 5, pp. 925–936, Oct. 2011.

[21] L. H. Tsoukalas and R. E. Uhrig, *Fuzzy and Neural Approaches in Engineering* (Wiley Series on Adaptive and Learning Systems for Signal Processing, Communications and Control). Hoboken, NJ, USA: Wiley, 1997.

[22] A. Halder, A. Konar, R. Mandal, A. Chakraborty, P. Bhowmik, N. R. Pal, and A. K. Nagar, "General and interval type-2 fuzzy face-space approach to emotion recognition," *IEEE Trans. Syst., Man, Cybern. Syst.*, vol. 43, no. 3, pp. 587–605, May 2013.

[23] W. Ding and D. Liang, "Modeling of a 6/4 switching reluctance motor using adaptive neural fuzzy inference system," *IEEE Trans. Magn.*, vol. 44, no. 7, pp. 1796–1804, Jul. 2008.

[24] W. Yu and X. Li, "Fuzzy identification using fuzzy neural networks with stable learning algorithms," *IEEE Trans. Fuzzy Syst.*, vol. 12, no. 3, pp. 411–420, Jun. 2004.

[25] M. Sreejeth, M. Singh, and P. Kumar, "Particle swarm optimisation in efficiency improvement of vector controlled surface mounted permanent magnet synchronous motor drive," *IET Power Electron.*, vol. 8, no. 5, pp. 760–769, May 2015.

[26] M. Iwasaki, N. Matsui, and K. Itoh, "Optimal design of robust vibration suppression controller using genetic algorithms," *IEEE Trans. Ind. Electron.*, vol. 51, no. 5, pp. 947-953, Oct. 2004.

[27] A. Lautin, *The Limbic Brain*. New York, NY, USA: Kluwer, 2002.

[28] M. Álvarez, R. Galán, F. Matía, D. Rodríguez-Losada, and A. Jiménez, "An emotional model for a guide robot," *IEEE Trans. Syst., Man, Cybern. A, Syst., Humans*, vol. 40, no. 5, pp. 982–992, Sep. 2010.

[29] C. D. Katsis, N. Katertsidis, G. Ganiatsas, and D. I. Fotiadis, "Toward emotion recognition in car-racing drivers: A biosignal processing approach," *IEEE Trans. Syst., Man, Cybern. A, Syst., Humans*, vol. 38, no. 3, pp. 502–512, May 2008.

[30] J. Moren and C. Balkenius, "A computational model of emotional learning in the amygdala," *Cybern. Syst.*, vol. 32, no. 6, pp. 611–636, 2000.

[31] C. Lucas, D. Shahmirzadi, and N. Sheikholeslami, "Introducing belbic: Brain emotional learning based intelligent controller," *Intell. Autom. Soft Comput.*, vol. 10, no. 1, pp. 11–21, Jan. 2004.

[32] M. A. Rahman, R. M. Milasi, C. Lucas, B. N. Araabi, and T. S. Radwan, "Implementation of emotional controller for interior permanent-magnet synchronous motor drive," *IEEE Trans. Ind. Appl.*, vol. 44, no. 5, pp. 1466–1476, Sep. 2008.

[33] M. A. Sharbafi, C. Lucas, and R. Daneshvar, "Motion control of omnidirectional three-wheel robots by brain-emotional-learning-based intelligent controller," *IEEE Trans. Syst., Man, Cybern. C, Appl. Rev.*, vol. 40, no. 6, pp. 630–638, Nov. 2010.

[34] M. Roshanaei, E. Vahedi, and C. Lucas, "Adaptive antenna applications by brain emotional learning based on intelligent controller," *IET Microw., Antennas Propag.*, vol. 4, no. 12, pp. 2247–2255, 2010.

[35] G. R. Markadeh, E. Daryabeigi, C. Lucas, and M. A. Rahman, "Speed and flux control of induction motors using emotional intelligent controller," *IEEE Trans. Ind. Appl.*, vol. 47, no. 3, pp. 1126–1135, May 2011.

[36] M. H. Soreshjani, G. A. Markadeh, E. Daryabeigi, N. R. Abjadi, and A. Kargar, "Application of brain emotional learning-based intelligent controller to power flow control with thyristor-controlled series capacitance," *IET Gener., Transmiss. Distrib.*, vol. 9, no. 14, pp. 1964–1976, Nov. 2015.

[37] R. E. Kandel, H. J. Schwartz, M. T. Jessell, A. S. Siegelbaum, and A. J. Hudspeth, *Principles of Neural Science*, 5th ed. New York, NY, USA: McGraw-Hill, 2013.

[38] *Opal-RT, OP 5600, HIL Box, Information Guide*. Accessed: Mar. 20, 2020. [Online]. Available: https://www.opal-rt.com

[39] D. J. Hill and P. J. Moylan, "Stability results for nonlinear feedback systems," *Automatica*, vol. 13, no. 4, pp. 377–382, Jul. 1977.

[40] P. Sarah and T. Day, *A Biologist's Guide to Mathematical Modeling in Ecology and Evolution*. Princeton, NJ, USA: Princeton Univ. Press, 2007.

[41] M. Qutubuddin and N. Yadaiah, "Modeling and implementation of brain emotional controller for permanent magnet synchronous motor drive," *Eng. Appl. Artif. Intell.*, vol. 60, pp. 193–203, Apr. 2017.

MD QUTUBUDDIN received the B.Tech. degree in electrical and electronics engineering, the M.Tech. degree in power electronics engineering, and the Ph.D. degree from JNTU Hyderabad, India, in 2008, 2012, and 2019, respectively. He has worked as a Senior Research Fellow with JNTUH Hyderabad. He has one year of industrial experience, five years of research experience, and four years of teaching experience. He is currently working as an Assistant Professor with the TKR College of Engineering and Technology, Hyderabad. His research interests include artificial techniques, electrical drives, brain modeling, and cognitive architectures.

TILAHUN KOCHITO GIBO was born in SNNPR, Ethiopia, in 1991. He received the B.Sc. degree in electrical and computer engineering (specialized in power engineering) from Hawassa University, Ethiopia, in 2015, and the M.Tech. degree in power electronics engineering from JNTUHCEH, Telangana, in 2020. He has two years of teaching and one year of industry experience. He is currently working as a Lecturer with the Electrical and Computer Engineering Department, Mizan-Tepi University, Ethopia. His research interests include power systems, power electronics and electrical drive systems, smart grid, and distributed generation.

RAJU S. BAPI (Senior Member, IEEE) received the B.E. degree in electrical engineering from Osmania University, Hyderabad, India, in 1983, and the M.S. degree in biomedical engineering and the Ph.D. degree in mathematical sciences computer science from The University of Texas at Arlington, USA. He worked with BHEL, India, the University of Plymouth, U.K., and the ATR Research Laboratory, Kyoto, Japan, before joining the University of Hyderabad, India, in 1999. He is currently a Professor with the Cognitive Science Laboratory, Kohli Centre for Intelligent Systems (KCIS), IIIT Hyderabad, India. His research interests include the practical applications of various neural network and machine learning techniques, investigation of biological neural architectures, neuroimaging, and cognitive modeling. He is a member of the Society for Neuroscience, USA, the Cognitive Science Society, USA, and the Association for Computing Machinery (ACM).

YADAIAH NARRI (Senior Member, IEEE) received the B.E. degree in electrical engineering from Osmania University, in 1988, the M.Tech. degree in control systems from IIT Kharagpur, India, in 1991, and the Ph.D. degree from JNTU Hyderabad, India, in 2000. He is currently a Professor of EEE with the Jawaharlal Nehru Technological University Hyderabad College of Engineering, India. He visited the University of Alberta, Edmonton, AB, Canada, as a Visiting Professor. He has 138 publications to his credit. He has completed three research and development projects and delivered more than 40 guest lectures as a key notes speaker. His research interests include adaptive control, artificial neural networks, fuzzy logic, nonlinear systems, and process control. He is a fellow of Institution Engineers, India, fellow of Institution of Electronics and Telecommunications Engineers, Life Member of the Systems Society of India, and Life Member of the Indian Society for Technical Education. He was awarded the 43rd SSI National Systems Gold Medal of 2019 by the Systems Society of India, the Meritorious State Teacher Award by the Government of Telangana, in 2015, the Engineer of Year Award of 2014 of Institution of Engineers of India by Andhra Pradesh Chapter, the Outstanding Reviewer Award of 2014 by Elsevier Publisher USA, and the Young Scientist Fellowship (YSF) of Andhra Pradesh State Council for Science and Technology, in 1999.